

Axial and equatorial H₂O molecules have also been proposed as ligands in dopamine- β -hydroxylase,⁴³ galactose oxidase,⁴⁴ and the type 2 copper sites in multicopper oxidases;⁴⁵ histidine imidazoles are known to be Cu(II) ligands in these enzymes as well.⁴³⁻⁴⁵ Despite the apparent structural similarities in the metal binding sites in these various Cu(II) containing enzymes, there is nevertheless considerable variation in the chemical and physical properties of the copper sites and in their probable catalytic roles.^{4,5,43-45} Copper ions in amine oxidases are not involved in substrate amine binding^{5,9} but evidently are essential for the oxidation of the substrate reduced enzyme by O₂.^{4-7,9,45,46} Since N₃⁻ and especially CN⁻ are effective amine oxidase inhibitors,

(43) Hasnain, S. S.; Diakun, G. P.; Knowles, P. F.; Binsted, N.; Garner, C. D.; Blackburn, N. J. *Biochem. J.* **1984**, *221*, 545-548.

(44) Kosman, D. J. In *Copper Proteins and Copper Enzymes*; Lontie, R., Ed.; CRC Press: Boca Raton, FL, 1984; Vol. 2, pp 1-26, and references cited therein.

(45) (a) Reinhammar, B.; Malmstrom, B. G. In *Copper Proteins*; Spiro, T. G., Ed.; Wiley: New York, 1981; pp 109-149. (b) See, also: *Copper Proteins and Copper Enzymes*; Lontie, R., Ed.; CRC Press: Boca Raton, FL, 1984; Vol. 3, for several reviews on multicopper oxidases.

(46) (a) Suzuki, S.; Sakurai, T.; Nakahara, A.; Manabe, T.; Okuyama, T. *Biochemistry* **1983**, *22*, 1630-1635. (b) Bellelli, A.; Brunori, M.; Finazzi-Agro, A.; Floris, G.; Giartosi, A.; Rinaldi, A. *Biochem. J.* **1985**, *232*, 923-926.

the ESE modulation results presented here suggest that the labile coordination position on at least one copper ion is important for catalysis. Its role may be a direct one, e.g., as in the proposal that equatorially coordinated hydroxide nucleophilically assists hydride transfer from the reduced organic cofactor to O₂,⁴⁷ or some electronic or structural property of the copper site, which is crucial for enzyme turnover, may be sensitive to equatorial ligand substitution.

Acknowledgment. We thank W. E. Blumberg, D. Zuckerman, and W. B. Mims for advice and technical assistance concerning the design of the pulsed EPR spectrometer used in these measurements and the analysis of ESEEM data. We also thank Cheryl Cote and Michele McGuirl for their dedicated and excellent technical assistance. That portion of this research carried out at Albert Einstein College of Medicine is supported by United States Public Health Service Grants RR-02583 and HL-13399. That portion of this research carried out at Amherst College is supported by the United States Public Health Service Grant GM-27659.

(47) (a) Kelly, I. D.; Knowles, P. F.; Yadav, K. O. S.; Bardsley, W. G.; Leff, P.; Waight, R. D. *Eur. J. Biochem.* **1981**, *114*, 133-138. (b) Yadav, K. O. S.; Knowles, P. F. *Eur. J. Biochem.* **1981**, *114*, 139-144.

Molecular Spectroscopy of High-Spin Co(II). Polarized Single Crystal Electronic Absorption Spectra of Structurally Defined Tetracoordinate Complexes with Sulfur-Donor Ligands^{1a}

Marvin W. Makinen,^{*†‡b} Susan C. Hill,[†] Michael Zeppezauer,[‡] Cindy L. Little,[†] and Jeremy K. Burdett[‡]

Contribution from the Department of Biochemistry and Molecular Biology, The University of Chicago, Cummings Life Science Center, Chicago, Illinois 60637, Fachbereich Biologische Chemie 15.2, Universität des Saarlandes, D-6600 Saarbrücken, Federal Republic of Germany, and Department of Chemistry, The University of Chicago, Chicago, Illinois 60637.

Received May 9, 1986

Abstract: The polarized single crystal electronic absorption spectra of active site specific Co²⁺-reconstituted horse liver alcohol dehydrogenase and of its binary inhibitor complexes formed with imidazole and pyrazole have been determined in the 42000-8000-cm⁻¹ range. There are, in general, three characteristic clusters of bands: low-intensity bands ($f \approx 0.001$) in the near-infrared near 10000 cm⁻¹, medium-intensity bands ($f \approx 0.01$) in the 20000-15000-cm⁻¹ region, and high-intensity bands ($f \approx 0.1$) in the 30000-25000-cm⁻¹ region. The spectra are assigned on the basis of the polarized single crystal spectrum of Co[SC(CH₃)₂CH₂NH₂]₂ and extended Hückel calculations of model complexes. The weak bands in the near-infrared region are assigned to ligand-field transitions of the high-spin Co²⁺ ion. The bands in the visible region are generally assigned also to ligand field transitions; however, the extended Hückel results predict a variety of ligand \rightarrow metal charge-transfer transitions through which significant intensity enhancement would occur. Of these ligand \rightarrow metal charge-transfer transitions, the orbitals of the sulfur ligands are responsible for absorption intensity in the visible region while the orbitals of the sulfur and nitrogen ligands account for absorption intensity in the near-ultraviolet. There is excellent agreement between the observed spectra of these complexes and that predicted by theory with respect to both relative intensity and energy of charge-transfer transitions in the visible and near-ultraviolet regions, and the spectra of the Co²⁺-enzyme can be accounted for by a chromophore of *accidental* axial symmetry in which the symmetry (z) axis bisects the S-Co-S valence angle of the active site metal ion complex. The agreement between predicted spectra calculated on the basis of molecular orbital models and the observed polarized absorption spectra provide a basis to extend this approach to the study of other small molecule Co²⁺ complexes and Co²⁺-reconstituted metalloenzymes and to characterize the active site metal ion in inhibitor complexes and reaction intermediates of liver alcohol dehydrogenase.

In a variety of Zn²⁺-containing metalloenzymes, the catalytically required tetracoordinate metal ion can be replaced by Co²⁺, often with complete retention of enzymatic activity.²⁻⁴ To probe metal ion function in these enzymes, the coordination structure and the intense electronic absorption properties of Co²⁺ substitutionally

incorporated into these enzymes have been an active focus of a large number of spectroscopic studies. Since most of these studies

^{*} The University of Chicago, Department of Biochemistry and Molecular Biology.

[†] Universität des Saarlandes.

[‡] The University of Chicago, Department of Chemistry.

(1) (a) This work was supported by grants of the NIH (AA 06374), NSF (PCM 77-13479), and the American Heart Association (77873) awarded to M.W.M., a grant of the Deutsche Forschungsgemeinschaft awarded to M.Z., and a grant of the NSF (DMR 80-19741) awarded to J.K.B. (b) Established Investigator of the American Heart Association for part of the tenure of this investigation.

(2) Lindskog, S. *Struct. Bonding (Berlin)* **1970**, *8*, 153-196.

have been carried out on solutions of metalloenzyme complexes, there has been little direct information about the molecular polarizations and the orbital origins of the complex patterns of spectral bands that are observed. To directly assign the principal molecular directions of transition moments of coordination complexes of Co^{2+} , it is necessary to analyze the polarized electronic absorption spectra of the metal ion incorporated into structurally defined sites in single crystals. While polarized absorption spectra of high-spin Co^{2+} substituted into host crystalline matrices have been reported, the analyses, carried out largely according to crystal field theory, have been limited to the near-infrared region and the visible region of the ${}^4\text{A}_2(\text{F}) \rightarrow {}^4\text{T}_1(\text{P})$ transition.⁵⁻¹¹ In no study have the intense charge-transfer transitions at higher energy been analyzed. Moreover, except for the study of Ballhausen and Liehr,¹² published over 25 years ago, relatively little attention has been directed to the analysis of the intensities of spectral bands of high-spin Co^{2+} in terms of molecular orbital theory. Since the higher energy charge-transfer bands are a direct monitor of metal-ligand interactions and are characteristically observed in the solution spectra of a number of Co^{2+} -substituted enzymes,^{2-4,13-16} their use to probe metal-substrate interactions in enzyme function may prove incisive in assigning the structural origins of metal function in catalysis.

Since an active area of investigation in our laboratories has been the structure and function of metalloenzymes, particularly with use of Co^{2+} as a probe of active site structure,¹⁶⁻²⁰ we have undertaken an extensive study of the electronic absorption properties of high-spin Co^{2+} in structurally defined sites. In this paper we report the polarized absorption spectra of active site specific Co^{2+} -reconstituted liver alcohol dehydrogenase^{19,20} and of a structurally defined tetracoordinate complex of high-spin Co^{2+} ²¹ as a small molecule model of the active site metal ion in the enzyme. Spectral bands are assigned on the basis of polarized single crystal absorption spectra collected over the 40000-6000 cm^{-1} range and on the basis of the extended Hückel molecular orbital structure calculated for model complexes. It is shown that the intensities of the prominent bands in the spectra can be adequately accounted for within the framework of extended Hückel

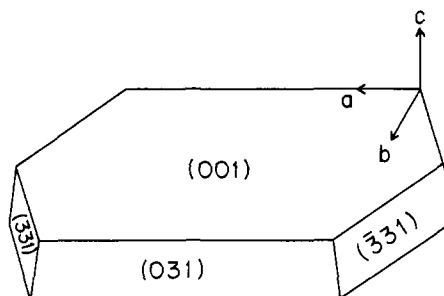


Figure 1. Clinographic projection of the $\text{C}222_1$ crystal of LADH illustrating the crystal axes and principal well-developed faces, as determined in this investigation.

theory and that the spectroscopic properties and molecular orbital structure of the small molecule complex can be directly applied to analyze the spectrum of the Co^{2+} -substituted enzyme.

Experimental Procedures

General. Bis(β -mercapto- β , β -dimethylethylamino)cobaltate(II) was incorporated into the host matrix of crystals of the isomorphous Zn^{2+} compound by cocrystallization under a nitrogen atmosphere, essentially according to the procedure described by Mastrapaolo et al.^{21,22} The following method was used: Aldrich Gold Label $\text{ZnSO}_4 \cdot 7\text{H}_2\text{O}$ (0.0145 g, 5×10^{-5} moles) and Baker Analyzed $\text{CoCl}_2 \cdot 6\text{H}_2\text{O}$ (0.0121 g, 5×10^{-5} mols) were dissolved in 7.5 mL of deoxygenated, distilled water heated to 60 °C. The solution was maintained in a nitrogen atmosphere and solid $\text{HSC}(\text{CH}_3)_2\text{CH}_2\text{NH}_2 \cdot \text{HCl}$ (0.0284 g, 20×10^{-5} mols) was added. After the ligand was dissolved, triethylamine was added to pH 9-10. The vessel containing the mixture of metal complexes was placed in a dewar containing water at 60 °C and allowed to cool to room temperature. Small, blue crystals suitable for microspectrophotometry formed within 1-2 h. After 7 h crystallization appeared complete, generally accompanied by appearance of a fluffy, white precipitate. Occasionally, crystals appeared greenish in color. It was assumed that these crystals were oxidized through inadvertent introduction of atmospheric oxygen during crystallization, and they were not employed for spectral studies. Suitable crystals with small amounts of the mother liquor were transferred to anaerobic cells for microspectrophotometry prepared from microscope slides and cover slips made of fused silica.

Crystalline LADH²³ was obtained from Boehringer-Mannheim. Crystals of the active site specific Co^{2+} -reconstituted enzyme were prepared and characterized as described by Maret et al.¹⁹ The extent of metal replacement in the crystals employed for this investigation was determined by analytical atomic absorption spectrometry to be 93% (1.86 g-atom of Co^{2+} per 80000 mol wt of the protein). This value was employed in the calculation of crystal extinction coefficients from polarized intensity data. No change in the spectral properties of the Co^{2+} -reconstituted enzyme was observed with storage of the crystals under a nitrogen atmosphere over a period of several months. Crystals of the native enzyme generally remain stable in aqueous alcoholic mixtures only near 0 °C.²⁴ In our studies we observed that crystals of the native and Co^{2+} -reconstituted enzyme remained intact at ambient room temperature for at least 12 h in 30% (v/v) *tert*-butyl alcohol buffered to pH 7 with 0.01 M Tes. This time was sufficient for collection of polarized optical density data.

Solution spectra were determined with either a Cary 14 or a Cary 15 spectrophotometer. For the active site specific Co^{2+} -reconstituted enzyme, estimation of isotropic extinction coefficients was based on the metal content determined analytically and the extinction coefficient of the Co^{2+} -substituted protein at 280 nm reported by Maret et al.¹⁹ Polarized single crystal absorption spectra were measured with the double-beam recording microspectrophotometer described previously.²⁵ For

(3) Makinen, M. W. In *Techniques and Topics in Bioinorganic Chemistry*; McAuliffe, C. A., Ed.; Macmillan Press: London, 1975; pp 3-106.

(4) Bertini, I.; Lucchinat, C. *Acc. Chem. Res.* **1983**, *16*, 272-279.

(5) (a) Ferguson, J. *J. Chem. Phys.* **1960**, *32*, 528-532. (b) Ferguson, J. *J. Chem. Phys.* **1963**, *39*, 116-128.

(6) Pappalardo, R.; Wood, D. L.; Linares, R. C., Jr. *J. Chem. Phys.* **1961**, *35*, 2041-2059.

(7) Weakliem, H. A. *J. Chem. Phys.* **1962**, *36*, 2117-2140.

(8) Ferguson, J.; Wood, D. L.; Knox, J. *J. Chem. Phys.* **1963**, *39*, 881-889.

(9) Holt, E. M.; Holt, S. L.; Watson, J. *J. Am. Chem. Soc.* **1970**, *92*, 2721-2724.

(10) Gerloch, M.; Kohl, J.; Lewis, J.; Urland, W. *J. Chem. Soc. A* **1970**, 3283-3296.

(11) Bertini, I.; Dapporto, P.; Gatteschi, D.; Scozzafava, A. *Inorg. Chem.* **1975**, *24*, 1639-1643.

(12) (a) Ballhausen, C. J.; Liehr, A. D. *J. Mol. Spectrosc.* **1958**, *2*, 342-360. (b) Ballhausen, C. J.; Liehr, A. D. *Ibid.* **1959**, *4*, 190-191.

(13) Latt, S. A.; Vallee, B. L. *Biochemistry* **1971**, *10*, 4263-4269.

(14) Speckhard, D. C.; Wu, F. Y. H.; Wu, C. W. *Biochemistry* **1977**, *16*, 5228-5234.

(15) Lindskog, S.; Ehrenberg, A. *J. Mol. Biol.* **1967**, *24*, 133-137.

(16) (a) Dunn, M. F.; Dietrich, H.; MacGibbon, K. H.; Koerber, S. C.; Zepezauer, M. *Biochemistry* **1982**, *21*, 354-363. (b) Andersson, I.; Burton, D. R.; Dietrich, H.; Maret, W.; Zepezauer, M. In *Metalloproteins*; Weser, U., Ed.; Goerg Theime Verlag: Stuttgart, FRG, 1979; pp 246-253.

(17) (a) Makinen, M. W.; Yim, M. B. *Proc. Natl. Acad. Sci. U.S.A.* **1981**, *78*, 6221-6225. (b) Makinen, M. W.; Maret, W.; Yim, M. B. *Proc. Natl. Acad. Sci. U.S.A.* **1983**, *80*, 2584-2588.

(18) (a) Kuo, L. C.; Makinen, M. W. *J. Biol. Chem.* **1982**, *257*, 24-27. (b) Kuo, L. C.; Fukuyama, J. M.; Makinen, M. W. *J. Mol. Biol.* **1983**, *163*, 63-105. (c) Makinen, M. W.; Kuo, L. C.; Yim, M. B.; Fukuyama, J. M.; Kim, J. E. *J. Am. Chem. Soc.* **1985**, *107*, 5245-5255. (d) Kuo, L. C.; Makinen, M. W. *Ibid.* **1985**, *107*, 5255-5261.

(19) Maret, W.; Andersson, I.; Dietrich, H.; Schneider-Bernlöhner, H.; Einarsson, R.; Zepezauer, M. *Eur. J. Biochem.* **1979**, *98*, 501-512.

(20) Schneider, G.; Eklund, H.; Cedergren-Zepezauer, E.; Zepezauer, M. *Proc. Natl. Acad. Sci. U.S.A.* **1983**, *80*, 5289-5293.

(21) Mastrapaolo, D.; Thich, J. A.; Potenza, J. A.; Shugar, H. J. *J. Am. Chem. Soc.* **1977**, *99*, 424-429.

(22) We are indebted to Professor H. J. Shugar for a generous supply of $\text{HSC}(\text{CH}_3)_2\text{CH}_2\text{NH}_2 \cdot \text{HCl}$ synthesized in his laboratory and to helpful guidance in the preparation of crystals.

(23) Abbreviations: EH, extended Hückel; LADH, (horse) liver alcohol dehydrogenase; correspondingly CoLADH designates the active site specific Co^{2+} -reconstituted enzyme as prepared by Zepezauer and co-workers;^{19,20} PR, polarization ratio defined as the ratio of two single crystal optical densities measured with incident light linearly polarized in each of two orthogonal directions specified by crystal symmetry; Tes, *N*-tris(hydroxymethyl)-methyl-2-aminoethanesulfonic acid.

(24) Zepezauer, E.; Söderberg, B. O.; Bränden, C. I.; Åkeson, Å.; Theorell, H. *Acta Chem. Scand.* **1967**, *21*, 1099-1101.

data collection in the near-infrared region, we have extended the photo-detection capability of this microspectrophotometer with use of a matched pair of photomultipliers (RCA 31004A) in the 700–950-nm range and a matched pair of PbS detectors (Series 1511, IR Industries, Inc., Waltham, MA) in the 900–1400-nm region, using modulated light detection.^{25c}

Optical Density Measurements of Single Crystals. The compound $\text{Co}[\text{SC}(\text{CH}_3)_2\text{CH}_2\text{NH}_2]_2$ and its isomorphous Zn^{2+} analogue crystallize in space group $C22_2$ with a tabular habit. Clinographic projections and structural and linear dichroism properties of this crystal have been described previously by Shugar and co-workers.²¹ In our polarized optical studies, identification of the (001) crystal face was made by conoscopic examination of crystals and by measurement of interfacial angles. Incorporation of Co^{2+} into the host matrix of crystals of the Zn^{2+} complex did not alter their habit or extinction axes.

LADH crystallizes in space group $C22_2$ with four dimeric units of the enzyme in the unit cell, and the only well developed face is (001).^{20,24} Ordinarily in polarized optical studies in our laboratory, we have converted crystal optical density data into crystal extinction coefficients.^{25–29} This conversion requires determination of crystal thickness by microscopic measurements, conveniently obtained by estimation of the length of the projection of oblique crystal faces onto the crystal plane that is perpendicular to the incident beam of plane-polarized light. A clinographic projection of a crystal of LADH is shown in Figure 1. Indexing of the oblique faces of the CoLADH crystal was carried out with large, well-formed crystals by measurement of the angles between the normals to the crystal planes when viewed along [001] and [010] with a two-circle goniometer and microscope attachment. Measurement of the projection of (031) onto the ab plane of the crystal then yields the crystal thickness since the dihedral interfacial angles are fixed by the crystallographic unit cell parameters. As for our earlier hemeprotein studies,^{25–29} the error in the measurement of the crystal thickness, estimated to be $\pm 10\%$, is the primary source of uncertainty in the calculation of crystal extinction coefficients.

Crystals of $\text{Zn}[\text{SC}(\text{CH}_3)_2\text{CH}_2\text{NH}_2]_2$ into which Co^{2+} was incorporated for spectroscopic studies were too thin for accurate measurement of such projections. Therefore, for the $\text{Co}[\text{SC}(\text{CH}_3)_2\text{CH}_2\text{NH}_2]_2$ complex, we have applied relationships based on geometrical considerations^{25,26,30} to calculate the isotropic spectrum from polarized crystal data, and we have normalized the peak (isotropic) extinction coefficient of the intense absorption band near 350 nm to coincide with that observed for the imidazole inhibitor complex of CoLADH. The ligand environment of the Co^{2+} ion in both systems corresponds to a CoS_2N_2 complex of approximate C_2 symmetry.

In an orthorhombic crystal the principal optic axes are coincident with the crystal axes.³¹ For all of the crystals employed in this investigation, spectroscopic measurements are made with plane polarized light incident normal to (001), the only well developed face of each crystal, so that the electric field vector of the incident beam of light is aligned parallel to either of the two crystal axes contained in this plane. Optical density measurements are reproducibly made to within ± 0.002 optical density units, and the spectra are constructed from data of several crystals of widely different thicknesses. We have examined the spectral properties of crystals of $\text{Zn}[\text{SC}(\text{CH}_3)_2\text{CH}_2\text{NH}_2]_2$ with different concentrations of the Co^{2+} ion incorporated into the host matrix. No change in the polarization properties was observed for Co^{2+} concentrations in the range of 0.05–0.5 mol fraction %. Therefore, we routinely employed crystals enriched with Co^{2+} up to 0.5 mol fraction % because of the intrinsically greater signal-to-noise ratio associated with data collection. On the other hand, in CoLADH crystals, the concentration of the active site Co^{2+} is fixed by an inert protein matrix. In this crystal there is only one active site metal ion per asymmetric unit, and the concentration of active sites

Table I. Atomic Coordinates (in Angstroms) and Atomic Numbering Scheme for $\text{Co}(\text{SCH}_3)_2(\text{NH}_3)_2$ ^{a,b}

group	atom	x	y	z
metal ion	Co	0.0000	0.0000	0.0000
SCH ₃	S	1.8984	0.0000	1.3424
	C	3.2964	0.0000	0.1802
	H ₁	2.9140	0.0000	-0.8555
NH ₃	H ₂	3.9121	0.9014	0.3452
	H ₃	3.9121	-0.9014	0.3452
	N	0.0000	1.6624	-1.1755
H ₂ O ^c	H ₄	0.0000	1.3799	-2.1743
	H ₅	0.8475	2.2274	-0.9757
	H ₆	-0.8475	2.2274	0.9757
	O _w	0.0000	-1.6583	-1.1726
	H _{w1}	0.7572	-2.1375	-1.5114
	H _{w2}	-0.7572	-2.1375	-1.5114

^a Atoms H₁ to H₃ are associated with the mercaptide ligand; atoms H₄ to H₆ are associated with the ammonia ligand. ^b Coordinates are given for purposes of brevity for only 2 of the ligands; coordinates for the S', N', C', and H_i atoms of the other two ligands can be generated by reflection across the yz plane for (SCH₃) and across the xz plane for (NH₃). ^c Coordinates of the atoms of the metal-bound water molecule for EH calculations of $\text{Co}(\text{SCH}_3)_2(\text{NH}_3)(\text{H}_2\text{O})$ in C_2 symmetry.

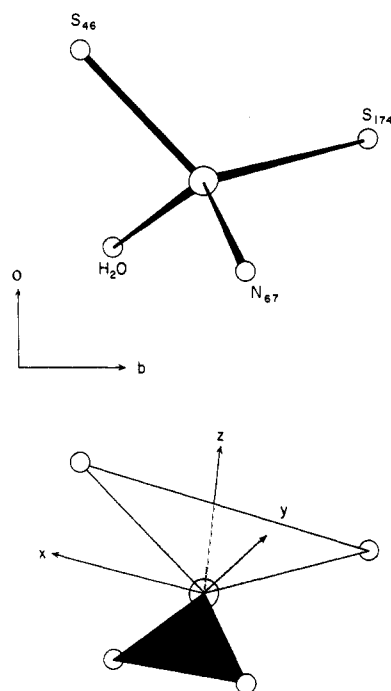


Figure 2. Projection of the immediate coordination environment of the active site metal ion of LADH onto the ab crystal face employed in polarized single crystal spectroscopic studies. The upper diagram illustrates the projection of the coordinate positions of the donor ligand atoms and the metal ion; the lower diagram illustrates the assignment of the molecular axis system and its projection onto the ab face of the crystal.

calculated from unit cell data^{20,24} is 0.0174 M. Because of the larger interchromophore distances, the electronic interactions between active sites are not sufficiently strong to perturb the crystal spectrum. This coincides directly with our previous experience in the study of the polarized single crystal absorption properties of heme complexes in proteins.^{25–29}

We have previously evaluated the effects of scattered light and crystal misalignment on polarization data.^{25a,b} For the microspectrophotometer employed in our laboratory, conditions are routinely maintained so that the ratio of the intensity of linearly polarized light to the intensity of depolarized or scattered light with crossed polarizers in the light beam is $\geq 1.5 \times 10^4$ in the absence of an absorbing medium. For the polarization properties of the crystals employed in this study, it is readily shown^{25a,b} that the effects of scattered light and crystal misalignment are less than the experimental uncertainty associated with single crystal optical density and dichroic ratio measurements.

Molecular Orbital Calculations. EH calculations of the electronic structures of $\text{Co}(\text{SCH}_3)_2(\text{NH}_3)_2$, $\text{Co}(\text{SCH}_3)_2(\text{NH}_3)(\text{H}_2\text{O})$, $\text{Co}(\text{SCH}_3)_2$ -

(25) (a) Churg, A. K.; Makinen, M. W. *J. Chem. Phys.* **1978**, *68*, 1913–1925. (b) Churg, A. K.; Makinen, M. W. *J. Chem. Phys.* **1978**, *69*, 2268. (c) Zelano, J. A.; Sigountos, J. G.; Makinen, M. W.; Sanders, H. *Rev. Sci. Instrum.* **1985**, *56*, 398–401.

(26) Makinen, M. W.; Churg, A. K. In *Physical Bioinorganic Chemistry Series. Iron-Porphyrins*; Lever, A. B. P., Gray, H. G., Eds.; Addison-Wesley: Reading, MA, 1983; Vol. 1, pp 143–235.

(27) Makinen, M. W.; Churg, A. K.; Glick, H. A. *Proc. Natl. Acad. Sci. U.S.A.* **1978**, *75*, 2291–2295.

(28) Churg, A. K.; Glick, H. A.; Zelano, J. A.; Makinen, M. W. In *Biochemical and Clinical Aspects of Oxygen*; Caughey, W. S., Ed.; Academic Press: New York, 1979; pp 125–139.

(29) Makinen, M. W.; Churg, A. K.; Shen, Y. Y.; Hill, S. C. In *Electron Transport and Oxygen Utilization*; Ho, C., Ed.; Elsevier-North Holland: New York, 1982; pp 101–109.

(30) Hofrichter, J.; Eaton, W. A. *Annu. Rev. Biophys. Bioeng.* **1976**, *5*, 511–560.

(31) Hartshorne, N. A.; Stuart, A. *Practical Optical Crystallography*, 2nd ed.; Arnold: London, 1969; Chapter 2, pp 47–108.

(imidazole)₂, and $\text{Co}(\text{SCH}_3)_2(\text{imidazole})(\text{H}_2\text{O})$ were carried out with use of the algorithm and computer program previously developed and applied by Hoffmann and co-workers.^{32,33} Symmetrized atomic coordinates of these complexes were based on crystallographic data or derived by calculation according to standard bond lengths and angles. Atomic coordinates are given in Table I. The EH parameters were identical with those employed by Summerville and Hoffmann³³ for metal ion complexes. For the Wolfsberg-Helmholz hamiltonian³⁴ employed in the calculations, the value of the interaction parameter was 1.75.

The Crystal and Molecular Structure of Liver Alcohol Dehydrogenase

Since the primary objective of this study is to identify features of the metal ion environment in the active site of CoLADH that are responsible for its electronic spectrum, we first describe the choice of molecular axes of the active site metal ion center in the native enzyme,^{20,35,36} as schematically illustrated in Figure 2. The active site metal ion is coordinated to the protein by the sulfhydryl groups of cysteine-174 and cysteine-46, and the imidazole side chain of histidine-57. A water molecule serves as the fourth ligand. In addition to the four metal-ligand bonds, there are long-range interactions (>5 Å) between the alcoholic OH groups of serine-48 and threonine-178. A second Zn^{2+} ion is also found in each subunit and is coordinated to the protein by four cysteine residues. This metal ion has no direct catalytic function and is not replaced by Co^{2+} when the active site specific Co^{2+} -reconstituted enzyme is prepared by the method of Zeppezauer and co-workers,^{19,20} as in this investigation.

In Figure 2 the relationships of the molecular axes to the crystal axes have been calculated on the basis of the atomic coordinates of the donor ligand atoms determined in difference Fourier studies of the ZnLADH-imidazole inhibitor complex,^{37,38} in which the N_1 atom of the imidazole ring has displaced the H_2O molecule. The molecular axes are labeled so that the z axis is formed by the intersection of the planes defined by the $\text{S}_{46}\text{-Zn-S}_{174}$ and the (imidazole) N-Zn-N_{67} valence angles. The x axis is constrained to lie in the $\text{S}_{46}\text{-Zn-S}_{174}$ plane and y is perpendicular to the x and z molecular axes. The calculated angle between the normals to these planes is 82° , indicating that the actual bonding relationships define very nearly mutually perpendicular planes. The structural relationships of the donor-ligand atoms to the metal ion illustrated in Figure 2 approximate the symmetry of the C_s point group wherein the mirror plane of symmetry contains the O-Zn-N_{67} valence angle. On the other hand, in the enzyme-imidazole complex, the configuration of the two liganding imidazole rings and the sulfhydryl groups confer an axis of approximate twofold rotational symmetry coincident with the z molecular axis. By examination of space-filling molecular models and by calculation, we have established that the imidazole groups cannot be positioned with resultant C_{2v} symmetry without unacceptably short, nonbonded contacts between the 2-H atoms of the imidazole ligands, and inspection of the difference Fourier results of the enzyme-imidazole inhibitor complex³⁷ shows that the two imidazole groups are not parallel to the yz plane. The structural relationships of the ligands to the metal ion may then be approximated by the symmetry requirements of the C_2 point group.

(32) (a) Hoffmann, R.; Lipscomb, W. N. *J. Chem. Phys.* **1962**, *36*, 3489-3496. (b) Hoffmann, R. *Ibid.* **1963**, *39*, 1397-1412.

(33) Summerville, R. H.; Hoffmann, R. *J. Am. Chem. Soc.* **1976**, *98*, 7240-7254.

(34) Wolfsberg, M.; Helmholz, N. *J. Chem. Phys.* **1952**, *20*, 837-843.

(35) Bränden, C. I.; Jörnvall, H.; Eklund, H.; Furugren, B. In *The Enzymes*, 3rd ed.; Boyer, P. D., Ed.; Academic Press: New York, 1975; Vol. XI, pp 103-190.

(36) Eklund, H.; Nordström, B.; Zeppezauer, E.; Söderlund, G.; Ohlsson, I.; Boiwe, T.; Söderberg, B. O.; Tapia, O.; Bränden, C. I. *J. Mol. Biol.* **1976**, *102*, 27-59.

(37) Boiwe, T.; Bränden, C. I. *Eur. J. Biochem.* **1977**, *77*, 173-179.

(38) During the course of this investigation, coordinates of the active site metal ion and donor ligand atoms derived from high resolution (2.0 Å) data with phase refinement were supplied to us by Professor C. I. Bränden. These new coordinates resulted in essentially no change in the calculated PR for x -, y -, and z -polarized transitions from that based on the coordinates listed in ref 37.

Table II. Relationships Derived According to Space Group and Crystal Habit To Calculate the Isotropic Spectrum of CoLADH Complexes from Polarized Single Crystal Extinction Coefficients^a

squared direction	l_z^2	0.1271
cosines of the	m_z^2	0.1446
z molecular axis	n_z^2	0.7283
based on X-ray		
crystal data ^b		
PR($b:a$) for accidentally degenerate transitions polarized in the molecular xy plane		$(1 - m_z^2)/(1 - l_z^2)$
PR($b:a$) for z -polarized nongenerate transitions		m_z^2/l_z^2
α_z^c		$\{(1 - m_z^2) - (1 - l_z^2)\text{PR}\} / \{(3l_z^2 - 1)\text{PR} - (3m_z^2 - 1)\}$
$\epsilon_{\text{calcd}}^d$		$\{\epsilon_a + \epsilon_b\} / \{3[1 - n_z^2\alpha_z - (1 - n_z^2)(1 - \alpha_z)/2]\}$

^a Derivations and calculation of optical properties are based on the assumption of an axially symmetric chromophore; see text for discussion. ^b The data in ref 37 were employed since the position of the metal-bound N_1 atom of the added imidazole ligand is better defined by X-ray data than is that of the water molecule in the native enzyme. ^c For calculation of α_z , the observed PR is employed. ^d Calculation of the isotropic spectrum is carried out under the assumption of the "oriented gas" approximation according to which $\epsilon_{\text{iso}} = (\epsilon_a + \epsilon_b + \epsilon_z)/3$ at any given wavelength λ . This approximation has been observed to hold rigorously in all hemeprotein studies^{25-30,39} to date. In these metalloprotein complexes the optical transitions are considerably more intense than those of tetracoordinate high-spin Co^{2+} . See text for discussion.

These geometries were accordingly employed for EH calculations.

Polarized Electronic Absorption Spectroscopy of CoLADH in Crystals

The molecular absorption of a chromophore in a crystal and the transformation of the molecular extinction tensor into the crystal coordinate axis system have been discussed by Hofrichter and Eaton.³⁰ For the C_{222_1} crystal of LADH with only one chromophore per asymmetric unit, the quantitative description of the absorption of linearly polarized light in the ac or bc crystal planes can be described by eq 1

$$\begin{aligned} \epsilon_a &= \epsilon_x \cos^2 \theta_{xa} + \epsilon_y \cos^2 \theta_{ya} + \epsilon_z \cos^2 \theta_{za} \\ \epsilon_b &= \epsilon_x \cos^2 \theta_{xb} + \epsilon_y \cos^2 \theta_{yb} + \epsilon_z \cos^2 \theta_{zb} \end{aligned} \quad (1)$$

where ϵ_a and ϵ_b are the crystal extinction coefficients with respect to the a and b axis polarized directions; ϵ_x , ϵ_y , and ϵ_z are the molecular extinction coefficients; and θ_{xa} , θ_{xb} , etc., denote the angle between the transition dipole moment for x -, y -, or z -polarized transitions and the a or b crystal axes, respectively. The habit of the crystal (cf., Figure 1) allows collection of polarized intensity data with respect to only two of the three orthogonal crystal axes. This circumstance and the low symmetry of the active site chromophore allow no further simplification of eq 1.

However, we have previously derived the relationships starting with eq 1 to calculate the solution spectrum from polarized crystal intensity data for an axially symmetric chromophore.^{25,26} These relationships are summarized in Table II. Since the orientation of the z molecular axis is uniquely defined under these conditions, the use of these equations in the analysis of the polarized crystal spectrum of CoLADH then permits a test for equivalence of x - and y -polarized transitions by comparison of the experimentally observed solution spectrum to the isotropic spectrum calculated from polarized optical data. Since the direction cosines l , m , n are independently defined by X-ray crystallographic data, agreement between the isotropic spectrum calculated from crystal data and the solution spectrum indicates that the effective electronic site symmetry of the chromophore is accidentally axial while a discrepancy between the calculated spectrum and the solution spectrum affirm that the effective site symmetry is lower. We

have previously employed this approach to define the effective site symmetry of heme complexes in proteins.²⁶ We shall demonstrate below that application of the relationships in Table II to the polarized crystal spectrum of the binary enzyme-imidazole complex reveals accidental equivalence of x and y . We then employ these results as a basis for the interpretation of the polarized crystal spectrum of the free CoLADH enzyme in which the metal ion is in a site of C_3 symmetry.

The parameter of most importance in the analysis of the crystal spectrum is the PR. This is the ratio of single crystal optical densities measured with incident light polarized in two orthogonal directions defined by crystal symmetry. Fluctuations of the PR with wavelength (the PR spectrum) reveal transition moment directions, deviations from true degeneracy, and the symmetry of perturbing influences of degenerate states. Diagnostic patterns in the PR spectrum of chromophores in oriented single crystals were first described by Eaton and Hochstrasser³⁹ and extended by us to include vibronic interactions,²⁶ and the reader should consult these references for further details of the PR spectrum that are of interpretative importance. With respect to the molecular axis system described in Figure 2, expressions for the PR($b:a$) of transitions polarized in the molecular x,y plane with accidental or true degeneracy (i.e., x and y equivalence) and of transitions polarized parallel to the z molecular axis are given in Table II. On the basis of the X-ray determined coordinates of the active site metal ion in LADH and its donor-ligand atoms,³⁷ PR($b:a$) values of 5.25 and 0.01 are predicted³⁸ for transitions of (apparent) x,y and z polarization, respectively. Furthermore, the crystal spectrum can be analyzed for the relative contributions of overlapping, apparent x,y - and z -polarized transitions since the fraction of z -polarized intensity (α_z , cf., Table II) can be calculated on the basis of the PR and the angle relationships between the molecular and crystal axis systems.

In the $\text{Co}[\text{SC}(\text{CH}_3)_2\text{CH}_2\text{NH}_2]_2$ crystal, the molecular z axis lies in the bc plane and is nearly perpendicular to the ab plane.²¹ This crystal structure consequently allows assignment of the principal molecular directions of transition moments simply by direct observation of transitions polarized along the b or a crystal axes. For optical bands polarized along the b axis, the transition moment lies parallel to the molecular z axis; correspondingly, for optical bands polarized along the a axis, the transition moment lies perpendicular to z . However, in this instance it is not feasible to obtain the spectrum of the complex in solution (also cf., ref 21) and a test for the local, effective symmetry of the chromophore as axial or nonaxial cannot be made as in the case of CoLADH. For $\text{Co}[\text{SC}(\text{CH}_3)_2\text{CH}_2\text{NH}_2]_2$, therefore, we identify transitions only as polarized parallel to or perpendicular to the molecular z axis.

Results and Discussion

A. Complexes of Active Site Specific Co^{2+} -Reconstituted LADH. The polarized single crystal absorption spectrum of the imidazole inhibitor complex of CoLADH is illustrated in Figure 3. The polarized crystal spectrum shows three prominent bands centered near 15 000, 18 750, and 27 100 cm^{-1} . The crystal spectrum resolves the band near 15 000 cm^{-1} into two closely overlapping components polarized in the a and b crystal directions while the band near 27 100 cm^{-1} is observed primarily in the b -crystal spectrum. In the ultraviolet region the polarization properties of the Co^{2+} enzyme reveal bands of weaker absorption intensity that are "hidden" in the solution spectrum, and two bands are exposed at 30 250 and 26 000 cm^{-1} in the a -polarized spectrum. A weak band is also identified at 31 500 cm^{-1} in the b -polarized spectrum. In the 40 000–33 000- cm^{-1} region, contributions to the spectrum arise from both the active site metal ion complex and the side chains of aromatic amino acid residues of the protein. No specific information can be obtained from this region because

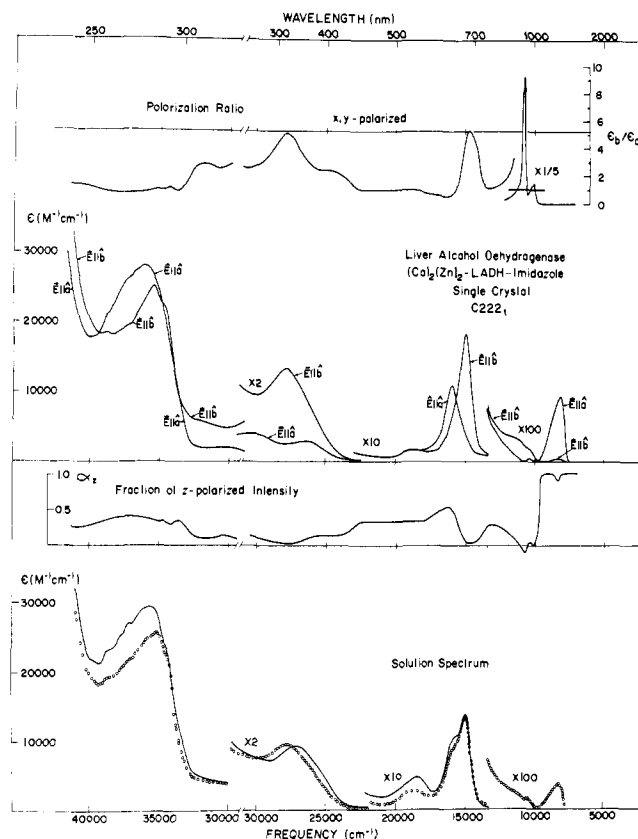


Figure 3. Polarized single crystal absorption spectrum of the CoLADH-imidazole complex with the electric field vector (E) of the beam of plane polarized light aligned parallel to either the b or a crystal axis. Crystals of CoLADH formed in aqueous *tert*-butyl alcohol^{19,20} were equilibrated with 0.01 M imidazole for several hours at ambient room temperature prior to data collection. In the upper part of the diagram is illustrated the PR($b:a$) spectrum. In the central region of the diagram is illustrated the wavelength variation of the fraction of z -polarized intensity (α_z) calculated according to relationships in Table II. The isotropic spectrum calculated from crystal data (ϵ_{calcd}) according to relationships in Table II and indicated by open circles in the lower part of the diagram is compared to the observed solution spectrum shown by the solid line spectrum. Sufficient CoLADH was not available to accurately record the solution spectrum in the near-infrared region. The solution spectrum is recorded for the complex buffered with 0.01 M Tes buffer to pH 7, as for the crystals.

of their many, different, overlapping contributions. In the near-infrared region, there are three bands of weak intensity that arise from ligand field transitions.

The PR reaches a value of 5.25 at the peak of the 15 000- cm^{-1} band while a sharp fluctuation to very low PR values is observed for the closely overlapping a -polarized component at 15 750 cm^{-1} . The dispersion in the PR spectrum indicates that these overlapping components are of different molecular polarization.^{26,39} The maximum value of the PR at 15 000 cm^{-1} coincides with that predicted on the basis of X-ray data for overlapping x - and y -polarized transitions of equal intensity, and there is a minimum in the calculated fraction of z -polarized intensity (α_z) near 15 000 cm^{-1} . The value of this parameter approaches a maximum of 0.5 for the 15 750- cm^{-1} band resolved in the a -crystal spectrum. We ascribe, therefore, the band at 15 000 cm^{-1} to transitions polarized in the x,y plane and the higher energy component at 15 750 cm^{-1} to z -polarized intensity. This analysis is confirmed by the excellent agreement of the isotropic spectrum calculated from crystal data with the observed solution spectrum.

The band centered at 18 750 cm^{-1} is associated with a deep trough in the PR spectrum. This reveals the presence of linearly polarized (nondegenerate) transitions of different molecular polarization from that of the 15 000- cm^{-1} band.^{26,39b} Since the minimum in the PR reaches a value of 0.90 only, rather than that of 0.01 predicted for purely z -polarized intensity, unresolved,

(39) (a) Eaton, W. A.; Hochstrasser, R. M. *J. Chem. Phys.* **1967**, *46*, 2533–2539. (b) Eaton, W. A.; Hochstrasser, R. M. *Ibid.* **1968**, *49*, 985–995.

(40) Sandorfy, C. *Electronic Spectra and Quantum Chemistry*; Prentice Hall: Englewood Cliffs, NY, 1964; Chapter 5, pp 98–100, and Chapter 8, pp 183–222.

overlapping bands of x or y polarization must also be present.

At the absorption maximum of the band at $27\,100\text{ cm}^{-1}$, the PR reaches a value of 5.10 in close agreement with the value of 5.25 predicted for (apparent) x,y polarization. There is also a corresponding minimum in the α_z spectrum. The crystal data, thus, demonstrate that this broad band arises primarily from overlapping x - and y -polarized transitions. In addition, in this spectral region two bands are exposed in the a -polarized spectrum at $26\,300$ and $30\,350\text{ cm}^{-1}$. These bands, therefore, must be of different molecular polarization, and we assign them to z -polarized transitions. Although a weak shoulder in the b -polarized spectrum is observed at $31\,500\text{ cm}^{-1}$, the overlapping absorption of the aromatic amino acid residues at higher energy obscures the true polarization of this weaker band. In the ultraviolet spectral region there is a noticeable discrepancy between the calculated isotropic spectrum and the observed solution spectrum. While the band shape and intensity are well preserved in the calculated spectrum, the absorption maximum is shifted to higher energy by $\sim 600\text{ cm}^{-1}$. We shall discuss later why this observation indicates that the environment of the Co^{2+} ion in the enzyme-imidazole complex formed in the crystal is not identical with that of the inhibitor complex in solution.

The near-infrared region of the spectrum shows a complicated pattern of overlapping bands arising from the ligand field transitions of the metal ion. In the polarized crystal spectrum, three bands are resolved, the lowest centered at 8200 cm^{-1} , while the other two overlap each other and are centered approximately at $10\,400$ and $11\,500\text{ cm}^{-1}$. The lowest energy band is readily designated as z polarized on the basis of its low PR (~ 0.1) and calculated fraction of z -polarized intensity (1.0). Precisely midway between the two higher energy bands, the PR undergoes a marked fluctuation, revealing the presence of two overlapping components, each of different molecular polarization and of approximately equal intensity. The value of the PR coincides midway with that predicted for x,y -polarized transitions and, thus, indicates that these bands must be due to transitions polarized along the molecular x and y axes.^{26,39} The α_z spectrum also reveals diffuse, overlapping, z -polarized components to the red of the visible absorption bands.

An essentially identical crystal spectrum with comparable polarization of the prominent bands in the visible and near-ultraviolet region was observed also for the CoLADH-pyrazole complex.

The polarized single crystal absorption spectrum of Co^{2+} -reconstituted LADH is illustrated in Figure 4. The spectrum is similar to that of the CoLADH-imidazole complex. The three prominent bands in the visible and near-ultraviolet regions centered at $15\,400$, $19\,100$, and $28\,800\text{ cm}^{-1}$ are of comparable intensity to those in the enzyme-imidazole complex. The band at $19\,100\text{ cm}^{-1}$ is readily ascribed to z -polarized transitions on the basis of its polarization properties while the symmetrical fluctuation of the PR spectrum associated with the band at $15\,400\text{ cm}^{-1}$ reveals the presence of two overlapping contributions of x and y molecular polarization. The α_z spectrum indicates a greater fraction of overlapping z -polarized intensity within the envelope of the $15\,400\text{-cm}^{-1}$ band than observed for the corresponding band in the spectrum of the enzyme-imidazole complex. The crystal spectrum also demonstrates that the broad band at $28\,800\text{ cm}^{-1}$ remains essentially (apparent) x,y,z polarized, and there are 500-cm^{-1} spacings in the PR spectrum. Comparable features in the polarized spectra of heme proteins, when correlated with resonance Raman spectra, suggest that they reveal the perturbation of metal-ligand vibrations on the electronic transitions.²⁶ The good agreement of the calculated isotropic spectrum with the solution spectrum confirms the assignment of these bands to overlapping (apparent) x,y - and z -polarized transitions, as in the spectrum of the enzyme-imidazole complex. However, in contrast to the polarized spectrum in Figure 3, there is close agreement in the ultraviolet region between the isotropic spectrum calculated from crystal data and the solution spectrum of CoLADH. This observation indicates that there is no significant change in the relative orientation of the aromatic amino acid residues and of

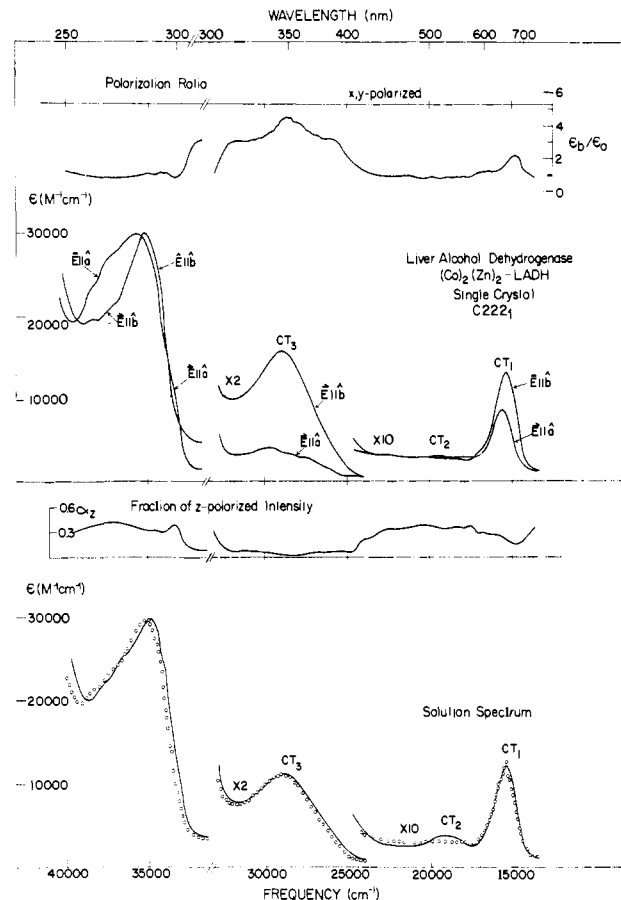


Figure 4. Polarized single crystal absorption spectrum of CoLADH. The crystal spectrum near $19\,000\text{ cm}^{-1}$ appears flattened in contrast to the small band in the solution spectrum. This is due to difficulty in finding sufficiently thick crystals of high optical quality to determine the polarized spectrum in this region. Symbols and labels are as designated in Figure 3.

the active site environment of the Co^{2+} ion in the protein in crystals and in solution. Since substitution of the metal ion is carried out in crystals of the enzyme,^{19,20} the coincidence of the two spectra means that the structure of the free, active-site specific Co^{2+} -reconstituted enzyme in the crystals is retained when dissolved.

The polarized single crystal spectrum of the ZnLADH-imidazole complex is illustrated in Figure 5. The isotropic spectrum calculated from crystal data is in good agreement with the solution spectrum. This observation indicates that the relative orientations of the aromatic amino acid side chains in the binary ZnLADH-imidazole complex remain unchanged in crystalline and solution states. The close agreement between the calculated isotropic spectrum and the solution spectrum also indicates that there are no interchromophore electronic interactions that perturb the crystal spectra. This observation, therefore, requires that the discrepancy in the ultraviolet region between the calculated isotropic spectrum and the solution spectrum of the imidazole inhibitor complex of CoLADH arises through structural perturbations induced by inhibitor binding in the crystal. It is probable that this structural perturbation effects only the relative orientation of the ligands in the active site and nearby protein residues.

B. The Polarized Single Crystal Absorption Spectrum of Bis- $[\beta$ -mercapto- β,β -dimethylethylamino]cobaltate(II). The polarized electronic absorption spectrum of $\text{Co}[\text{SC}(\text{CH}_3)_2\text{CH}_2\text{NH}_2]_2$ incorporated to 0.5 mol fraction % into the host crystal matrix of the isostructural Zn^{2+} compound is shown in Figure 6. The spectrum in the $20\,000$ – $15\,000\text{-cm}^{-1}$ region is essentially identical with that previously described by Mastrapaolo et al.²¹ The studies here extend the spectrum into the ultraviolet and near-infrared regions and provide more precise estimates of the intensities of the optical bands. Although intensity data could be collected with plane polarized light incident normal to only the (001) face of

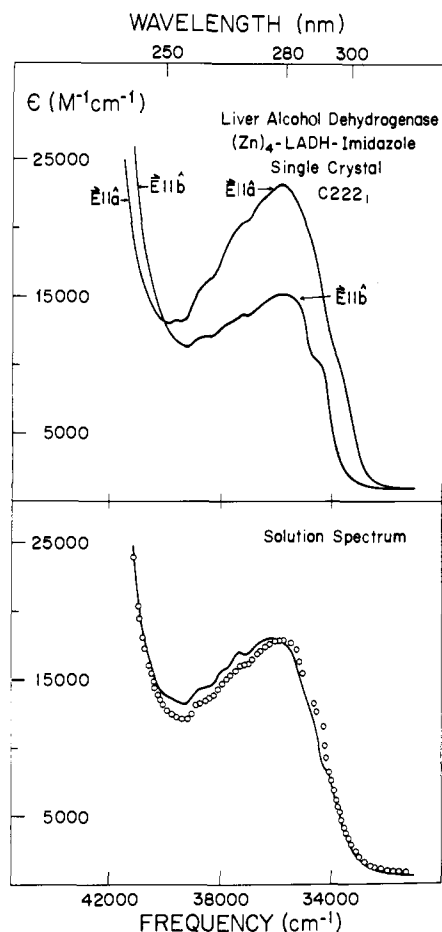


Figure 5. Polarized single crystal absorption spectrum of the binary imidazole complex³⁷ of native ZnLADH. Crystals of native ZnLADH were treated similarly to those of CoLADH, as described in Figure 3 for spectral data collection. Symbols and labels as in Figure 3.

this crystal, the structural relationships of the complex to the crystal axes provide a particularly informative orientation of the metal ion with its four donor-ligand atoms. The z axis of the complex, bisecting the S-Co-S' valence angle and formed by the intersection of the S-Co-S' and N-Co-N' planes, is contained in the bc crystal plane. The molecular x and y axes correspondingly are contained in the ac crystal plane. The crystal

structure, thus, ensures that the polarized absorption spectrum collected with the electric field vector aligned parallel to the b axis arises from z -polarized transitions while the spectrum collected with the electric field vector aligned parallel to the a axis arises from transitions polarized perpendicular to the molecular z axis. As seen in the visible region of the spectrum, the band at $17\,650\text{ cm}^{-1}$ that is resolved in the b -crystal spectrum exhibits also a weak projection onto the a -crystal axis. This observation indicates that the molecular z axis that is determined by the local electronic structure of the Co^{2+} site is not precisely parallel to the bc crystal plane and does not correspond exactly to that calculated on the basis of the X-ray defined atomic coordinates. According to the observed PR at the absorption maximum, we estimate that the deviation of the molecular z axis from the crystallographic bc plane is $\leq 7^\circ$. This deviation may be due in part to the circumstance that the dihedral angle defined by the planes of the S-Co-S' and N-Co-N' valence angles is 78.8° , and therefore, the complex does not exhibit exact C_{2v} symmetry. Furthermore, there may be small distortions of the ligand environment of the metal ion that are not resolved within the uncertainties associated with the X-ray determined structural parameters.

There are three regions of the spectrum that exhibit highly anisotropic absorption. In the near-infrared region, the absorption intensity is observed primarily in the a -polarized spectrum and, therefore, is of x or y molecular polarization. The lowest energy region of the broad, near-infrared band shows two weak, z -polarized features at $10\,500$ and $9\,100\text{ cm}^{-1}$ that are detected in the b -crystal spectrum. The visible region is resolved into two bands. A band centered at $15\,300\text{ cm}^{-1}$ appears in the a -crystal spectrum and must arise from x - or y -polarized transitions. The broader band centered at $17\,650\text{ cm}^{-1}$ appears in the b -crystal spectrum and is unambiguously assigned to z -polarized intensity. At somewhat higher energy between $25\,000$ and $20\,000\text{ cm}^{-1}$ there is weak absorption intensity that is nearly isotropically polarized. The ultraviolet region shows two prominent bands in the a -crystal spectrum centered near $29\,250$ and $35\,000\text{ cm}^{-1}$ while weaker features are observed in the b -crystal spectrum at $27\,900$ and $38\,200\text{ cm}^{-1}$. As for bands at lower energy, the features in the a -crystal spectrum must belong to x - or y -polarized transitions whereas the features in the b -crystal spectrum must arise from z -polarized transitions.

C. Extended Hückel Molecular Orbital Calculations of the Active Site Metal Ion Complex in CoLADH. For the assignment of the orbital origins and the transition moment directions of the optical bands observed in the spectra of complexes of CoLADH and of $\text{Co}[\text{SC}(\text{CH}_3)_2\text{CH}_2\text{NH}_2]_2$, we have carried out EH calculations of the electronic structure of $\text{Co}(\text{SCH}_3)_2(\text{NH}_3)_2$ in C_{2v}

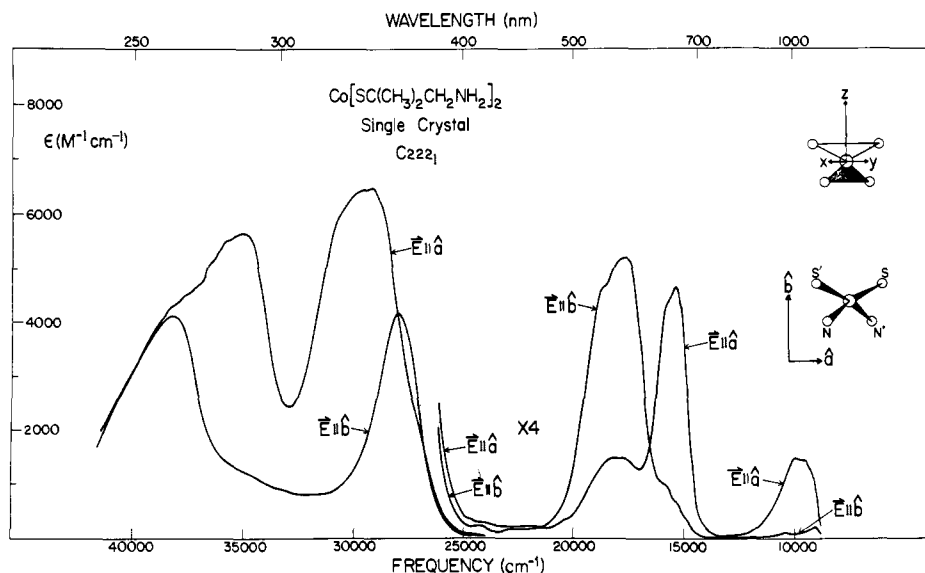


Figure 6. Polarized single crystal absorption spectrum of $\text{Co}_{0.5}\text{Zn}_{0.5}[\text{SC}(\text{CH}_3)_2\text{CH}_2\text{NH}_2]_2$ with the electric field vector (\mathbf{E}) of incident plane polarized light aligned parallel to the b - and a -crystal axes. In the right-hand position of the diagram is illustrated the projection of the positions of the ligand donor atoms and the metal ion and of the molecular axis system onto the ab face of the crystal.

Table III. Eigenvalues and Eigenvectors Calculated for $\text{Co}(\text{SCH}_3)_2(\text{NH}_3)_2$ in C_{2v} Symmetry^a

orbital no. and occupancy	energy (eV)	symmetry (orbital type)	principal atomic orbital coefficients
(19) ¹	-11.21	$b_2(d_{yz})$	$-0.82d_{yz} - 0.11\text{Co}(p_y) + 0.23[\text{N}(p_z) + \text{N}'(p_z)] + 0.35[\text{N}(p_y) + \text{N}'(p_y)] + 0.25[\text{S}(p_y) + \text{S}'(p_y)]$
(20) ¹	-11.28	$b_1(d_{xz})$	$0.76d_{xz} - 0.16\text{Co}(p_x) + 0.29[\text{S}(p_z) - \text{S}'(p_z)] + 0.39[\text{S}(p_x) + \text{S}'(p_x)] + 0.11[\text{H}_3 - \text{H}_3']$
(21) ¹	-11.34	$a_1(d_{x^2-y^2})$	$-0.79d_{x^2-y^2} + 0.13\text{Co}(p_z) - 0.20[\text{N}(p_z) + \text{N}'(p_z)] + 0.23[\text{N}(p_y) - \text{N}'(p_y)] - 0.31[\text{S}(p_z) + \text{S}'(p_z)] + 0.23[\text{S}'(p_x) - \text{S}(p_x)]$
(22) ²	-12.26	$a_2(d_{xy})$	$-0.71d_{xy} + 0.51[\text{S}(p_y) - \text{S}'(p_y)] + 0.10[\text{H}_1' - \text{H}_2 + \text{H}_3 - \text{H}_2']$
(23) ²	-12.73	$a_1(d_{z^2})$	$0.96d_{z^2} + 0.11d_{x^2-y^2} - 0.15[\text{S}(p_z) - \text{S}'(p_z)]$
(24) ²	-13.07	b_2	$0.22d_{yz} + 0.11\text{Co}(p_y) + 0.61[\text{S}(p_y) + \text{S}'(p_y)] + 0.13[\text{C}(p_y) + \text{C}'(p_y) + \text{N}(p_y) + \text{N}'(p_y)] + 0.15[\text{H}_1 - \text{H}_1'] - 0.15[\text{H}_2 - \text{H}_2']$
(25) ²	-13.30	a_2	$0.70d_{xy} + 0.45[\text{S}(p_y) - \text{S}'(p_y)] - 0.10[\text{C}(p_y) - \text{C}'(p_y)] + 0.11[\text{H}_1' + \text{H}_1] - 0.11[\text{H}_2 + \text{H}_2']$
(26) ²	-13.45	a_1	$0.22d_{z^2} - 0.34d_{x^2-y^2} + 0.44[\text{S}(p_z) + \text{S}'(p_z)] + 0.28[\text{S}(p_x) - \text{S}'(p_x)] + 0.20[\text{N}(p_y) - \text{N}'(p_y)] - 0.13[\text{N}(p_z) + \text{N}'(p_z)] + 0.18[\text{H}_3 + \text{H}_3']$
(27) ²	-13.60	b_1	$-0.53d_{xz} + 0.50[\text{S}(p_z) - \text{S}'(p_z)] + 0.13[\text{S}(p_x) + \text{S}(p_x)] - 0.15[\text{C}(p_z) - \text{C}'(p_z)] + 0.12[\text{S}(3s) - \text{S}'(3s)] + 0.17[\text{H}_3 - \text{H}_3']$
(28) ²	-14.53	a_1	$0.49d_{x^2-y^2} + 0.43[\text{N}(p_y) - \text{N}'(p_y)] - 0.30[\text{N}(p_z) - \text{N}'(p_z)]$
(29) ²	-14.58	b_1	$-0.35d_{xz} + 0.41[\text{S}(p_x) + \text{S}'(p_x)] - 0.22[\text{S}(p_z) - \text{S}'(p_z)] - 0.26[\text{C}(p_x) + \text{C}'(p_x)] + 0.15[\text{C}(p_z) - \text{C}'(p_z)] - 0.10[\text{S}(3s) - \text{S}'(3s)] - 0.11[\text{H}_1 - \text{H}_1'] - 0.11[\text{H}_2 - \text{H}_2']$
(30) ²	-14.72	b_2	$-0.54d_{yz} - 0.41[\text{N}(p_y) + \text{N}'(p_y)] + 0.30[\text{N}(p_z) - \text{N}'(p_z)]$
(31) ²	-14.86	a_1	$0.15d_{z^2} + 0.10\text{Co}(4s) - 0.38[\text{S}(p_x) - \text{S}'(p_x)] + 0.27[\text{S}(p_z) + \text{S}'(p_z)] + 0.27[\text{C}(p_x) - \text{C}'(p_x)] - 0.17[\text{C}(p_z) + \text{C}'(p_z)] + 0.11[\text{H}_1 + \text{H}_1' + \text{H}_2 + \text{H}_2']$
(32) ²	-15.76	b_1	$0.27[\text{C}(p_z) - \text{C}'(p_z)] + 0.22[\text{C}(p_x) + \text{C}'(p_x)] + 0.16[\text{S}(p_z) - \text{S}'(p_z)] + 0.14[\text{S}(p_x) + \text{S}'(p_x)] - 0.32[\text{H}_3 - \text{H}_3'] + 0.16[\text{H}_1 - \text{H}_1' + \text{H}_2 - \text{H}_2']$
(33) ²	-15.77	a_2	$-0.35[\text{C}(p_y) - \text{C}'(p_y)] - 0.21[\text{S}(p_y) - \text{S}'(p_y)] + 0.28[\text{H}_1 + \text{H}_1'] - 0.28[\text{H}_2 + \text{H}_2']$
(34) ²	-15.77	b_2	$-0.35[\text{C}(p_y) + \text{C}'(p_y)] - 0.21[\text{S}(p_y) + \text{S}'(p_y)] - 0.28[\text{H}_1' + \text{H}_1] + 0.28[\text{H}_2 - \text{H}_2']$
(35) ²	-15.82	a_1	$0.29[\text{C}(p_z) + \text{C}'(p_z)] + 0.19[\text{C}(p_x) - \text{C}'(p_x)] + 0.16[\text{S}(p_z) + \text{S}'(p_z)] + 0.16[\text{S}(p_x) - \text{S}'(p_x)] - 0.32[\text{H}_3 + \text{H}_3'] + 0.15[\text{H}_1 + \text{H}_1' + \text{H}_2 + \text{H}_2']$
(36) ²	-16.43	b_2	$-0.37[\text{N}(p_z) - \text{N}'(p_z)] - 0.26[\text{N}(p_y) + \text{N}'(p_y)] + 0.31[\text{H}_4 - \text{H}_4'] - 0.16[\text{H}_5 + \text{H}_5' + \text{H}_6 - \text{H}_6']$
(37) ²	-16.52	b_1	$0.44[\text{N}(p_x) + \text{N}'(p_x)] + 0.27[\text{H}_5 + \text{H}_5'] - 0.27[\text{H}_6 + \text{H}_6']$
(38) ²	-16.53	a_2	$0.44[\text{N}(p_x) - \text{N}'(p_x)] - 0.27[\text{H}_5 + \text{H}_5' + \text{H}_6 + \text{H}_6']$
(39) ²	-16.60	a_1	$-0.36[\text{N}(p_z) + \text{N}'(p_z)] - 0.25[\text{N}(p_y) - \text{N}'(p_y)] + 0.31[\text{H}_4 + \text{H}_4'] - 0.16[\text{H}_5 + \text{H}_5' + \text{H}_6 + \text{H}_6']$

^aThe atomic numbering scheme and coordinates are listed in Table I.

symmetry as the simplest model compound and have compared these results to the molecular orbital structure calculated with imidazole substituted for NH_3 . For the model compound $\text{Co}(\text{SCH}_3)_2(\text{NH}_3)_2$ we have listed the eigenvalues and eigenvectors of the EH hamiltonian in Table III. The orbitals 19–23 have $\geq 50\%$ origin from the pure metal d orbitals with varying contributions largely from nitrogen or sulfur p orbitals. Of these, the highest energy orbitals 19, 20, and 21 are singly occupied and the electronic configuration corresponds, therefore, to that of a high-spin ($S = 3/2$) d^7 ion. Of the filled orbitals at lower energy, orbitals 28 and 30 have significant contributions from nitrogen p orbitals while the remaining orbitals have predominantly contributions from sulfur p orbitals. Orbital 32 and all orbitals of lower energy have no contributions from metal d orbitals and are comprised largely of sulfur and carbon p orbitals with approximately 10% of their composition deriving from hydrogen s orbitals. The lowest energy, unfilled orbitals are found approximately 11 eV above orbital 19. Therefore, the unfilled orbitals are not expected to contribute to any optical transitions that are observed in the spectrum of $\text{Co}[\text{SC}(\text{CH}_3)_2\text{CH}_2\text{NH}_2]_2$ below $40\,000\text{ cm}^{-1}$. For this reason, they have not been included in Table III.

On the basis of the wave functions in Table III, we have estimated the oscillator strengths of the quartet-allowed one-electron promotions from the lower, doubly occupied orbitals into the predominantly metal d-like orbitals 19–21. The oscillator strengths are estimated (cf., ref 40) by the relationship

$$f = (1.085 \times 10^{-5})\omega \cdot Q^2 \cdot G$$

where ω (in units of cm^{-1}) is the EH calculated energy separation of the lower and upper orbitals involved in the transition, G is the degeneracy ($1/2$ for quartet-allowed transitions into orbitals 19–21), and Q (in units of \AA) is defined by the integral $\int \phi_i r \phi_f d\tau$ where ϕ_i is the lower EH molecular orbital and ϕ_f is the upper orbital. The value of Q is approximated by the integral $\int \phi_{ir} r \phi_{fs} d\tau$ where r and s specify the atomic orbital contributions to the molecular orbitals ϕ_i and ϕ_f . This integral has a nonzero value for $r = s$ and is evaluated by the summation $\sum c_{ir} c_{fr} r_r$ where c_{ir} and c_{fr} are the EH calculated coefficients of the atomic orbitals in the lower and upper molecular orbitals and r_r is the vector distance from the Co^{2+} ion at the origin to the atom on which the

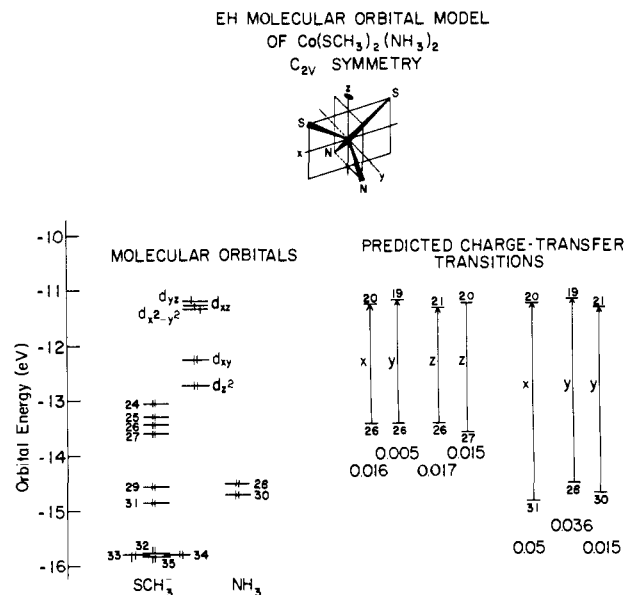


Figure 7. Illustration of the EH orbital structure of $\text{Co}(\text{SCH}_3)_2(\text{NH}_3)_2$ in C_{2v} symmetry and the most intense predicted charge-transfer transitions in the visible and near-ultraviolet regions. For the predicted charge-transfer transitions the upper and lower molecular orbitals, polarizations, and calculated oscillator strengths are illustrated on the right-hand side.

atomic orbital ϕ_i is centered. The oscillator strengths of transitions into the molecular orbitals 19, 20, and 21 of $\text{Co}(\text{SCH}_3)_2(\text{NH}_3)_2$ that are expected to contribute significantly to the optical spectrum are schematically illustrated in Figure 7. As is immediately evident in Figure 7, there is good correspondence between the observed and calculated transition energies and relative intensities in the visible and ultraviolet regions.

The orbital promotions that can account for the spectrum are clustered into two groups. One cluster is seen in the visible region with predominantly z- and x-polarized intensity. These transitions occur by one-electron promotions from orbitals of mixed metal

and sulfur composition into the higher lying orbitals of predominantly metal d-like character. We note that the polarized optical spectrum shows a z-polarized band at 17650 cm^{-1} . The band at 15300 cm^{-1} can be designated only as x- (or y-) polarized since analysis of this crystal spectrum permits only identification of transitions polarized parallel to or perpendicular to z. The calculated oscillator strengths in the visible region, as shown in Figure 7, predict nonequivalence of x- and y-polarized intensity. This circumstance for the model compound stands in contrast to the essentially "axial" spectrum observed for the CoLADH-imidazole complex.

In the ultraviolet region the summed intensity calculated for y-polarized transitions near 27000 cm^{-1} is equivalent to that of the intense x-polarized transition. For both types of transitions the intensity is due to promotions from orbitals of predominantly sulfur and nitrogen p character into the metal d-like orbitals 19–21. In Figure 6 an intense band centered at 29250 cm^{-1} is observed in the a-crystal spectrum. The observed polarization of this band is consistent with a group of closely spaced x- and y-polarized transitions. There are also weak z-polarized transitions predicted in the ultraviolet region. In the polarized crystal spectrum of $\text{Co}[\text{SC}(\text{CH}_3)_2\text{CH}_2\text{NH}_2]_2$, the bands observed in the b-crystal spectrum near 28000 cm^{-1} can arise only from z-polarized transitions. The relative integrated areas of the b- and a-polarized bands are consistent with the greater calculated oscillator strengths of the x- and y-polarized transitions near 27000 cm^{-1} .

It is evident that application of a simple EH model adequately reproduces the transition energies and relative intensities. More sophisticated methods for metal ion coordination complexes, as for instance developed by Zerner and co-workers,^{41,42} undoubtedly would account more accurately in matching calculated with observed spectral intensities, and the approximation employed here to estimate oscillator strengths cannot be applied to transitions of the ligand field type. These transitions are predicted to lie in the near-infrared and probably account for the weaker, broad bands observed near 10000 cm^{-1} , as seen in Figures 3 and 6. Of these transitions the promotions $23 \rightarrow 20$ and $22 \rightarrow 19$ are x polarized while $23 \rightarrow 19$ and $22 \rightarrow 20$ are y polarized. The promotion $23 \rightarrow 21$ is the only z-polarized d-d transition. On the whole, the calculated orbital energy separation suggests that the z-polarized transition will be at slightly lower energy than the x- or y-polarized transitions. This relative ordering is in good agreement with the observed polarization of the absorption intensity of $\text{Co}[\text{SC}(\text{CH}_3)_2\text{CH}_2\text{NH}_2]_2$ in the near-infrared region.

To complete the comparison of the orbital structure of the model compound $\text{Co}[\text{SC}(\text{CH}_3)_2\text{CH}_2\text{NH}_2]_2$ to the active site metal ion of CoLADH, we have carried out EH calculations of $\text{Co}(\text{SC}(\text{H}_3)_2(\text{NH}_3)(\text{H}_2\text{O}))$, $\text{Co}(\text{SCH}_3)_2(\text{imidazole})_2$, and $\text{Co}(\text{SCH}_3)_2(\text{imidazole})(\text{H}_2\text{O})$. We summarize the results for the latter two model systems only, for the calculated orbital patterns are essentially identical with those of $\text{Co}(\text{SCH}_3)_2(\text{NH}_3)_2$ and $\text{Co}(\text{SCH}_3)_2(\text{N}-\text{H}_3)(\text{H}_2\text{O})$, respectively, except that the total number of orbitals is increased and there are low-lying π^* orbitals of the imidazole groups that may be involved in electronic transitions in the ultraviolet. In Figure 8 we have compared the pattern of oscillator strengths of predicted transitions of the $\text{Co}(\text{SCH}_3)_2(\text{imidazole})_2$ complex calculated on the basis of the EH derived molecular orbitals to the spectrum of the CoLADH-imidazole complex in solution.⁴³ In general, there is good agreement between predicted and observed polarizations, energies, and relative intensities of the optical bands, as observed for $\text{Co}(\text{SC}(\text{CH}_3)_2\text{CH}_2\text{NH}_2]_2$. It is of interest to note also that there is near equivalence of predicted x- and y-polarized absorption intensity in the visible region, in agreement with the analysis of crystal data showing an (accidentally) "axial" spectrum. The direct correspondence of calculated and observed spectra indicates that the orbital promotions giving rise to the optical transitions of complexes of CoLADH

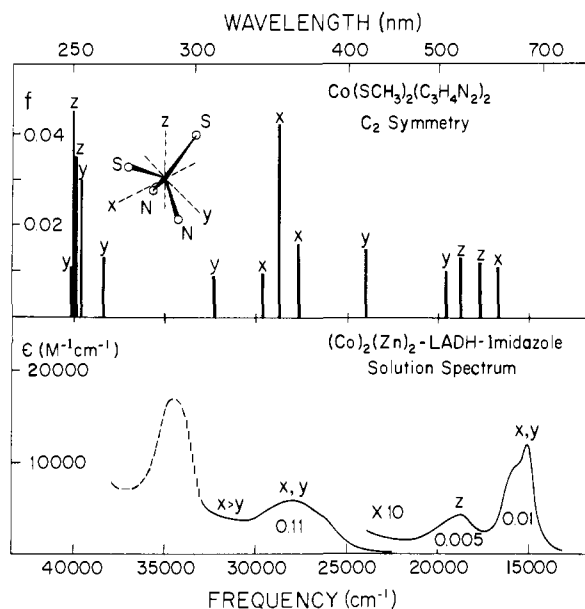


Figure 8. Comparison of the oscillator strengths and polarizations of transitions in the visible and ultraviolet regions predicted on the basis of the EH orbital structure of $\text{Co}(\text{SCH}_3)_2(\text{imidazole})_2$ in C_2 symmetry to the solution spectrum of the CoLADH-imidazole complex. In the lower panel for each prominent optical band, the polarization and oscillator strength calculated from the solution spectrum are indicated. The dotted part of the spectrum indicates the region in which overlapping transitions of both aromatic protein residues and of the active site metal ion complex are expected.

are essentially identical with those of the more simple, model compounds.

D. General Conclusions. In the analysis of the PR and polarized absorption spectra of complexes of CoLADH, the underlying simplification that we have made is that the chromophore is axially symmetric and that the spectrum has origin only in nondegenerate transitions polarized along the molecular z axis or in transitions that are accidentally degenerate and polarized in the molecular x,y plane. This simplification was applied because the habit of the enzyme crystal restricts the collection of polarized absorption data to the (001) plane, and therefore, a three-dimensional analysis of the anisotropy of the absorption of plane polarized light could not be carried out. As we have earlier outlined,^{25,26} agreement between the calculated and observed spectra indicates that the metal-ligand complex behaves like an axially symmetric chromophore while discrepancies between the observed and calculated isotropic spectrum reveal the nonequivalence of x- and y-polarized intensity and deviations from assumed axial symmetry. This approach, thus, provides a means to determine the effective site symmetry of the chromophore and to compare the origins of optical transitions for related chromophores independent of crystal structure.

Application of this approach to the assignment of bands in the polarized crystal spectrum of the imidazole inhibitor complex of CoLADH (Figure 3) has been particularly informative. In the C_{22v} crystal of CoLADH, the a- and b-polarized crystal spectra arise from overlapping contributions because of the chromophore orientation in the asymmetric unit. For each complex of CoLADH, comparison of the calculated and observed solution spectrum revealed excellent agreement in the visible region, indicating that the assumption of an axially symmetric chromophore is a good approximation since both band shape and intensities were well matched. Furthermore, for CoLADH the intensity and shape of the bands in the near-ultraviolet region are accurately predicted. This agreement, thus, provides the basis for applying the results of EH calculations of highly symmetrized model complexes to assign the orbital origins of the spectra of complexes of the metal-reconstituted enzyme in which the coordination geometry of active site ligands is considerably more distorted. The success of the results directly contradicts assertions⁴⁴ that the electronic

(41) Bacon, A. D.; Zerner, M. C. *Theor. Chim. Acta* **1979**, *53*, 21–54.

(42) Loew, G. H.; Zerner, M. C. *J. Am. Chem. Soc.* **1980**, *102*, 1815.

(43) Tables of the eigenvalues and eigenvectors and of the principal orbital promotions that account for the spectra of the imidazole inhibitor complex and of the free enzyme are available upon written request.

properties of metal ion centers in proteins and enzymes cannot be adequately described on the basis of idealized model systems.

The optical spectra of coordination compounds may be classified in general into ligand field bands and charge-transfer bands. The visible absorption spectra of high-spin Co^{2+} complexes in low-symmetry sites have been interpreted only in terms of intense ligand field transitions.⁴⁻¹¹ This tradition has been continued in textbooks of the spectroscopy of inorganic coordination complexes in which the intensity in the visible region of spectra of high-spin tetrahedral Co^{2+} complexes is ascribed to ligand field transitions with 3d-4p mixing.^{45,46} The classical study of Ballhausen and Liehr¹² demonstrated that d-p mixing due to the tetrahedral crystal field is insufficient as a mechanism of intensity to account for the visible absorption spectra of tetrahedral complexes of high-spin Co^{2+} . Similarly, on the basis of the EH molecular orbital model, metal p orbitals are not involved in optical transitions. As shown in Table III, there are small contributions of metal p functions in the highest singly occupied orbitals 19, 20, and 21. However, the lower energy, doubly occupied orbital 26, from which transitions best account for the intensity in the visible region, has no metal p orbital contribution. Of the three possible quartet-allowed electron promotions from orbital 24 with a small fraction of metal p function, the transition 24 \rightarrow 20 is symmetry forbidden; the value of Q is zero for 24 \rightarrow 19; and the one-electron promotion 24 \rightarrow 21 yields an estimated oscillator strength of 7.5×10^{-4} , insignificant in comparison to those from orbital 26 with mixing of only ligand and metal d wave functions. Moreover, the orbitals

28, 30, and 31, which account best for the more intense, near-ultraviolet bands, have no metal p contributions. The results of our EH calculations show that the most intense optical bands in the visible and near-ultraviolet regions can be accounted for best from the mixing of either sulfur or nitrogen orbitals into the lower and upper molecular orbitals associated with optical transitions and that not only the bands in the near-ultraviolet but also the bands in the visible region are predominantly of charge-transfer character. On the other hand, the weak bands in the near-infrared region are clearly consistent according to both energy and intensity with assignment to transitions involving primarily the metal d orbitals.

It is, moreover, of interest to note that the choice of parameters for our EH calculations to predict energies and relative intensities of ligand \rightarrow metal charge-transfer transitions was restricted to the set generally employed by others^{32,33} without further adjustment to obtain agreement between theory and experiment. Also, coefficients for the double- ζ expansion of the Slater exponents for 3d functions³³ were not employed. The EH results yielded in each case remarkably good agreement with observed spectra, consistent with our previous experience in the assignment of heme optical spectra on the basis of polarized single crystal spectra and EH molecular orbital models.²⁵⁻²⁹ This approach of assigning the orbital origins of the spectrum on the combined basis of polarized single crystal spectroscopic data and molecular orbital models, therefore, should be suitable to investigate further the influence of changes in metal coordination environment, particularly with respect to donor ligand atoms and coordination number as may occur in the enzyme-catalyzed reaction.^{17,47}

Registry No. $\text{Co}(\text{SCH}_3)_2(\text{NH}_3)_2$, 108122-73-2; $\text{Co}(\text{SCH}_3)_2(\text{N}-\text{H}_3)(\text{H}_2\text{O})$, 108122-74-3; $\text{Co}(\text{SCH}_3)_2(\text{imidazole})_2$, 108122-75-4; $\text{Co}(\text{SCH}_3)_2(\text{imidazole})(\text{H}_2\text{O})$, 108122-76-5.

(44) (a) Vallee, B. L.; Williams, R. J. P. *Proc. Natl. Acad. Sci. U.S.A.* **1968**, *59*, 498-502. (b) Williams, R. J. P. *Cold Spring Harbor Symp. Quant. Biol.* **1972**, *36*, 53-62. (c) Vallee, B. L.; Galdes, A. In *Advances in Enzymology and Related Areas of Molecular Biology*; Meister, A., Ed.; Wiley: New York, 1984; pp 283-430.

(45) Lever, A. B. P. *Inorganic Electronic Spectroscopy*; Elsevier: New York, 1984; pp 480-505.

(46) Williams, A. F. *A Theoretical Approach to Inorganic Chemistry*; Springer Verlag: Berlin, 1979; Chapter 4, pp 132-158.

(47) Yim, M. B.; Wells, G. B.; Kuo, L. C.; Makinen, M. W. In *Frontiers in Bioinorganic Chemistry*; Xavier, A. V., Ed.; VCH Verlagsgesellschaft: Weinheim, FRG, 1986; pp 562-570.

Polyhedral Clusters in Solids: The Electronic Structure of Pentlandite

Jeremy K. Burdett* and Gordon J. Miller

Contribution from the Department of Chemistry, The University of Chicago, Chicago, Illinois 60637. Received September 15, 1986

Abstract: The pentlandite structures are transition-metal sulfides that contain distinguishable metal atom cubes and exist only for certain combinations of the Fe group elements, Co_9S_8 being the only known binary phase. In this paper, we assemble the structure from the naked cube cluster after demonstrating the inadequacies of a ligand field analysis in rationalizing its physical properties. Molecular analogues also exist that exhibit different structural and physical features based upon the influence of a few orbitals near the HOMO-LUMO gap. We stress the importance of the octahedrally coordinated metals to the Co_8S_8 framework and how it contributes to the stability of Co_9S_8 . Finally, the relative stabilities of various structural alternatives, both observed and hypothetical, for transition-metal sulfides of stoichiometry MS with tetrahedrally coordinated metal atoms are examined as a function of d-count by using the method of moments.

Transition-metal sulfides provide the crystal chemist a number of diverse structural types to study.¹ Many have no counterparts among the oxide compounds, e.g., the pyrites and marcasites, the NiAs structure, and the layered MoS_2 , CdCl_2 , and CdI_2 structure types. Like intermetallic compounds, their chemical formulas may not depict normal chemical valences, as in Co_9S_8 , $\text{Rh}_{17}\text{Se}_{15}$, or

N_3S_2 . Such rather unique phases exhibit a variety of physical properties—metallic lustre, reflectivity, and electronic conductivity. The crystal structures of several transition-metal sulfides show close metal-metal distances, indicative of metal-metal bonding to some extent. These arise from the specific site occupations in the sulfide matrix or by distortions of an "ideal" high-symmetry arrangement of atoms to one of lower symmetry, e.g., the NiAs to MnP transition.

In this paper we shall examine the electronic properties of a class of sulfide compounds called π -phases or pentlandites,² with

(1) Comprehensive discussions of metal sulfides occur in the following: (a) Wuensch, B. J. In *Reviews in Mineralogy*; Ribbe, P., Ed.; Mineralogical Society of America: Washington, DC, 1982; Vol. 1, Sulfide Mineralogy. (b) Hulliger, F. *Struct. Bonding* **1968**, *4*, 83. (c) Jellinek, F. In *Inorganic Sulfur Chemistry*; Nickless, G., Ed.; Elsevier: Amsterdam; p 669. (d) Vaughan, D. J.; Craig, J. R. *Mineral Chemistry of Metal Sulfides*; Cambridge University Press: New York, 1978.

(2) (a) Knop, O.; Ibrahim, M. A. *Can. J. Chem.* **1961**, *39*, 297. (b) Knop, O. *Chem. Ind.* **1962**, 739.